

Self-assembled FePt nanodot arrays with mono-dispersion and -orientation

Zheng Gai

Condensed Matter Sciences Division, Oak Ridge National Laboratory, Oak Ridge, Tennessee 37831 and
Department of Physics, State Key Laboratory for Mesoscopic Physics, Peking University, Beijing
100871, People's Republic of China

J. Y. Howe

Metals & Ceramics Division, Oak Ridge National Laboratory, Oak Ridge, Tennessee 37831

Jiandong Guo

Department of Physics and Astronomy, The University of Tennessee, Knoxville, Tennessee 37996

D. A. Blom

Metals & Ceramics Division, Oak Ridge National Laboratory, Oak Ridge, Tennessee 37831

E. W. Plummer

Condensed Matter Sciences Division, Oak Ridge National Laboratory, Oak Ridge, Tennessee 37831 and
Department of Physics and Astronomy, The University of Tennessee, Knoxville, Tennessee 37996

J. Shen^{a)}

Condensed Matter Sciences Division, Oak Ridge National Laboratory, Oak Ridge, Tennessee 37831

(Received 20 September 2004; accepted 19 November 2004; published online 4 January 2005)

For self-assembled nanodots, the ultimate dream is to simultaneously achieve tunable uniformity in size, spatial distribution, chemical composition, and crystallographic orientation. By utilizing the Volmer–Weber growth mode in thin film epitaxy, we have grown self-assembled two-dimensional arrays of FePt alloy nanodots that are uniform in size, chemical composition, and *are all crystallographically aligned*. These dot assemblies are ferromagnetic at room temperature and can be easily transferred onto other templates without destroying the size and orientation uniformity. © 2005 American Institute of Physics. [DOI: 10.1063/1.1849849]

Self-assembled nanodots that are uniform in size, spatial distribution, chemical composition, and crystallographic orientation are highly desirable for the applications of catalysis¹ and high-density data storage.^{2,3} So far both chemical and physical methods have been employed for nanodot growth. The chemical method has become very attractive after the successful demonstration by Sun *et al.* to synthesize FePt dot assembly with uniform size, spatial order, and uniform chemical composition.⁴ The very nature of this chemical synthesis method, however, did not allow for the dots to be crystallographically aligned. On the other hand, the physical method of thin film epitaxy has been known as a convenient way to control the crystallographic orientation using a desired substrate. To apply this technique for nanodots, one must utilize the Volmer–Weber (VW) growth mode. The challenge is to identify a proper substrate that allows one to simultaneously achieve tunable uniformity in size, spatial distribution, chemical composition, and crystallographic orientation.

We used (001)-oriented NaCl single crystal substrate to grow FePt nanodots by co-deposition of Fe and Pt onto the NaCl(001) surface in an ultrahigh vacuum (UHV) system with a base pressure of better than 1×10^{-10} Torr.⁵ The morphology of the samples was studied *in situ* by an Omicron variable-temperature atomic force microscopy (VT-AFM). The samples were then capped with carbon film for *ex situ* transmission electron microscopy (TEM) study.⁶ The chemical composition and the size of the FePt dots can be tuned by controlling the growth parameters that include Fe versus Pt

deposition rate, the substrate temperature, and the total dosage of Fe and Pt. The substrate temperature plays an important role in defining the size, the density, and the size distribution of the dots. In general, the dot size increases and the dot density decreases with increasing temperature. The size uniformity can only be achieved in a narrow temperature window, with the optimal temperature being around 590 K. Figure 1(a) shows a 600 nm \times 600 nm AFM image of the FePt alloy dots grown at 585 K on a NaCl(100) substrate with a nominal thickness of 1.3 Monolayers (ML). Similar to the nanodots of pure Fe,⁷ the FePt alloy dots were also formed directly on the NaCl(001) surface without a wetting layer. As shown by the marked line scan, the dots are about 5–6 nm in height. While the values of the heights are precise for the AFM measurement, the lateral dimensions of the dots are overestimated due to the tip effect. However, based on the information of the shape, the height, and the density of the dots, plus the predetermined total dosage, we estimate that the real lateral size of the dots in Fig. 1(a) is around 7 nm. This has been confirmed by further TEM analysis, as shown in Fig. 2(a), which yields precise information on the shape as well as the lateral sizes of the dots. Interestingly, dots shown in the TEM images have rectangular shape. Figures 1(b) and 1(c) are the height and lateral size distributions of the dots along with the corresponding Gaussian fits. Consistent with the line profile and the lateral size estimation, the centers of the Gaussian fits of the height, the breadth (the shortest dimension across the center), and the length (the longest dimension across the center) distributions of the dots appear at 5.5, 5.8, and 8.0 nm, respectively. The distributions of the width are very narrow. The standard deviation, Δh

^{a)}Electronic mail: shenj@ornl.gov

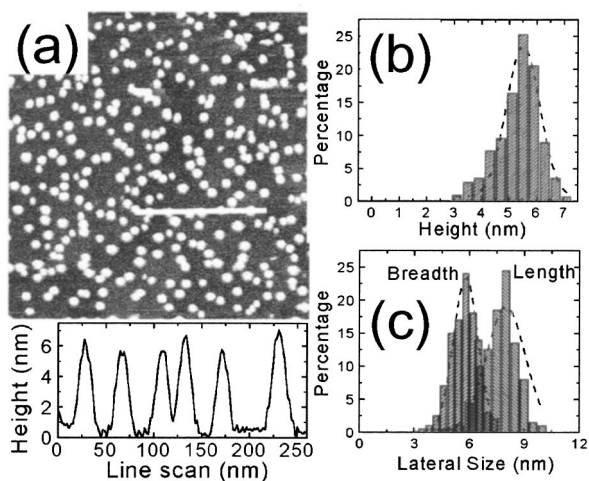


FIG. 1. (a) *In situ* AFM image of FePt alloy dots grown on cleaved NaCl(001) surface with a nominal thickness of 1.3 ML at substrate temperature of 585 K, the scan area is 600 nm \times 600 nm. The line profile at the bottom of the image shows the uniformity of the height and width of the dots. (b) and (c) are the height and lateral diameter distributions (length and breadth) of the alloy dots. The height distribution was from the AFM data, while the lateral size distributions were from the TEM measurements. The dashed lines are the corresponding Gaussian fits of the distributions.

$=(\langle h^2 \rangle - \langle h \rangle^2)^{1/2}$, of the height, breadth, and length distributions are only 0.65, 0.72, and 1.08 nm, respectively, which are 12%, 12.5%, and 13.5% of the average height and lateral size values. Such narrow dispersions are remarkable considering the fact that VW growth generally yields much broader size distributions even for clusters formed by single elements.²

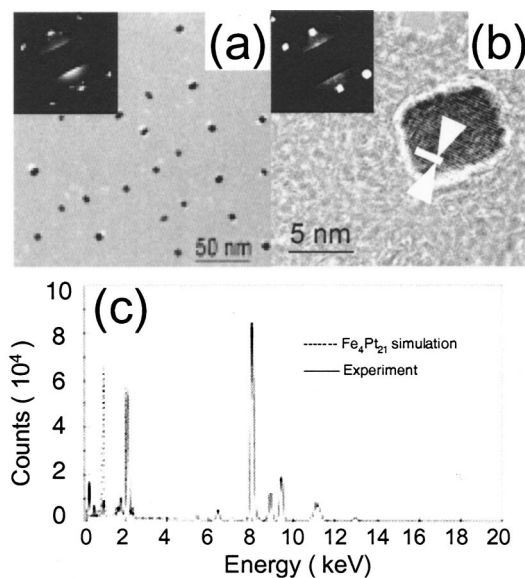


FIG. 2. TEM micrographs of the FePt dots assembly in Fig. 1 after it was transferred to a carbon thin film. (a) Typical image of the dots assembly, which is similar to the AFM images in the sense of the density and lateral size after deconvolution. Note that the rectangular dots are all aligned up along the crystalline orientation of NaCl (001); (b) HRTEM image of a single dot revealed the (200) lattice fringes, the distance between the white lines is 0.193 nm, i.e., the lattice constant is 0.39 nm; the micro-electron diffraction patterns from a group of dots as (a) (see the text) and single dots as (b) are shown as insets in (a) and (b), respectively. (c) EDS spectra of experimental and simulated patterns of the alloy nanodots. The simulation were carried out by assuming Fe:Pt ratio as 4:21.

The most striking observation comes from the TEM study of the dots assembly, which convincingly shows that all the dots are crystallographically aligned in both the vertical and lateral directions even after being transferred from the NaCl (100) surfaces to the carbon films. Figure 2(a) clearly displays the rectangular shape of the dots and their unanimous orientation, i.e., edges of those rectangles are all surprisingly aligned in the same orientations, which reveals that all of the dots are strongly bonded to the substrate during the growth. High resolution TEM images of all dots [as an example, see Fig. 2(b)] show the same kind of lattice fringes of (200) plane, which belongs to group *Pm-3m* (221), with a lattice constant of 0.39 nm. The most direct evidence of the epitaxial growth came from the microelectron diffraction analysis.⁸ The insets of Figs. 2(a) and 2(b) are the diffraction patterns from a group of dots and a single dot, respectively, indexed as {220} and {200} spots. The pattern for the single dot is a single set of diffraction, indicating that the dots are single crystals. Meanwhile the pattern from a group of dots [the inset of Fig. 2(a)] was taken from an area (200 nm in diameter) that contains 25 dots. This represents a set of similar diffraction patterns with less than 5° misalignment to each other, which we believe originates from the tilt or deformation of the thin carbon film (less than 5 nm). We thus conclude that all of the dots are crystallographically aligned.

Combining the diffraction and the energy dispersive spectroscopy analysis, the chemical composition of the particular dots assembly is confirmed to be Fe₄Pt₂₁ for each single dot. Energy dispersive spectra (EDS) were collected from individual dots to determine the chemical composition. The experimental EDS spectra from the dots is presented as solid line in Fig. 2(c). The simulated spectra with the Fe and Pt ratio of 4:21 is also shown in the same figure as a dotted line, which fit well to the experimental spectra.⁹

By using vicinal NaCl(001) substrates, we can spatially align the FePt alloy dots with uniform size, crystalline orientation, and chemical composition. Such vicinal NaCl substrates were prepared by polishing small angle misoriented NaCl(001) crystals with water-methanol mixture,¹⁰ followed by an annealing at 860 K in UHV chamber for about 40 min. Uniform terrace-step morphology with monolayer high steps can be formed on whole surfaces. The width of the terraces can be tuned by the miscut angles. When Fe and Pt atoms are co-evaporated onto stepped surfaces, the strong tendency for step decoration drives the FePt dots to the step edges, spatially ordered alloy nanodots assembly are formed. As an example, Fig. 3 shows a 1 μ m \times 1 μ m AFM image of the FePt alloy dots array grown on a 3.0° miscut NaCl(001) crystal. As shown in the inset of Fig. 3, both the sizes of the dots and the distances between the dots' chains are very uniform.

The Volmer-Weber growth mode for FePt on NaCl(001) can be rationalized by the large surface free energy imbalance between the substrate and adsorbates (2.48 J/m² for both Fe and Pt versus 0.18 J/m² for NaCl). Very recently, the size uniformity of single element dots grown in VW growth mode was interpreted by a phenomenological mean-field theory⁷ and a more detailed theoretical model¹¹ outlining the competition between the self-energy of a dot and the energy of the strong dot-dot interactions. In the FePt alloy dots system, the presence of the second element complicates the situation by introducing a new energy term which reflects the selection of the chemical composition into the self-energy of

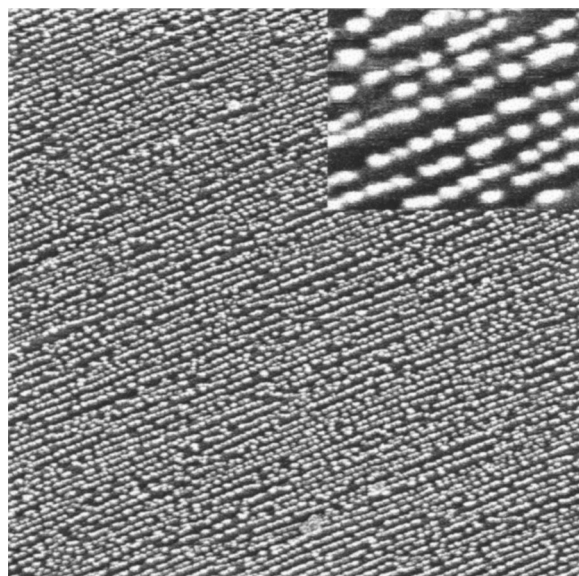


FIG. 3. *In situ* AFM images of spatially ordered FePt alloy dots grown on stepped NaCl(001) surface with nominal thickness of 1.3 ML at substrate temperature of 585 K. Scan area $1\ \mu\text{m} \times 1\ \mu\text{m}$. The inset picture is a close-up of the dots chains, $110\ \text{nm} \times 90\ \text{nm}$.

the dots. Nevertheless, the complexity of the current system does not change the generic behavior of which a local energy minimum presents at the observed optimal size and chemical composition. The amazing mono-orientation of the dots likely originates from epitaxy of FePt alloy on NaCl(001). Assuming the Fe or Pt atoms in the FePt alloy lattice register the Na and Cl sites alternately on the (001) surface, the mismatch between the two lattices is 3%. Based on these generic arguments, we thus anticipate that NaCl(001) can be used as a common template to grow dot assemblies that have similar uniformity in size, chemical composition, and crystalline orientation.

The self-assembled two-dimensional array of FePt alloy nanodots is ferromagnetic at room temperature. Figure 4 shows the results of the *ex situ* superconducting quantum interference device (SQUID) magnetometer measurement of the dots assembly which was capped with NaCl before it was taken out from the UHV chamber. The zero field cool and field cool magnetization data as a function of temperature in an external field of 50 Oe show a dispersion up to 300 K, indicating that the superparamagnetic blocking temperature of the nanodots assembly should be higher than room temperature. This is consistent with the results that hysteresis loops persist at all temperature ranges we can reach (5–300 K). Note that with our experimental setup, we can easily get all kinds of alloy dots assemblies by just tuning one or more growth parameters, including the dosage for changing the dots size, growth temperature for tuning the uniformity and density of the dot assemblies, substrate tilt angle for periodicity, the growth rates ratio of elements for modifying the alloy composition, and also the elements combinations. This

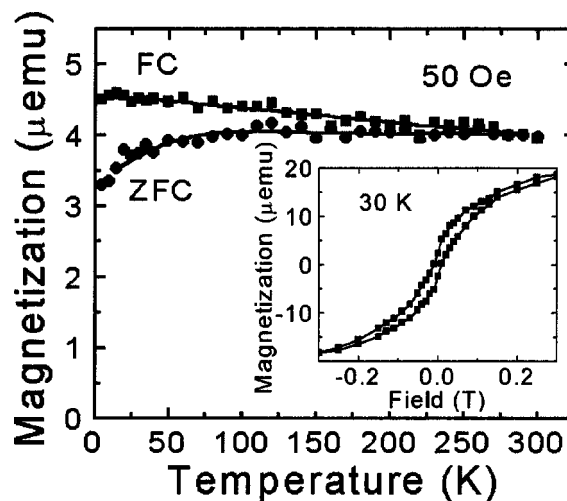


FIG. 4. Zero field cool (circles) and field cool (square) temperature dependence of the magnetization of the NaCl(001) supported $\text{Fe}_4\text{Pt}_{21}$ alloy dots. The curves are measured at the field of 50 Oe. The inset is a typical hysteresis acquired at 30 K by SQUID magnetometer.

advantage makes the systematic study of the magnetic properties of alloy nanodots assemblies possible, and makes it much easier to search for new magnetic materials.

This work was supported by Oak Ridge National Laboratory (ORNL), managed by UT-Battelle, LLC for the U. S. Department of Energy under Contract No. DE-AC05-00OR22725, and by the U.S. National Science Foundation under Contract No. DMR 0105232.

¹C. R. Henry, *Surf. Sci. Rep.* **31**, 235 (1998).

²P. Moriarty, *Rep. Prog. Phys.* **64**, 297 (2001).

³V. A. Shchukin and D. Bimberg, *Rev. Mod. Phys.* **71**, 1125 (1999), and references therein.

⁴S. Sun, C. B. Murray, D. Weller, L. Folks, and A. Moser, *Science* **287**, 1989 (2000).

⁵The iron and platinum were evaporated from Fe and Pt wires (5N purity) heated by electron beam bombardment. The NaCl single crystal substrates were cleaved in air, then were immediately loaded into the UHV chamber and were annealed to 530 K for 1 h to remove surface contamination prior to the experiments.

⁶TEM was carried out using a Hitachi HF2000 field emission TEM at 200 kV. The nanodots assemblies along with the thin carbon capping layer were detached from the substrate by immersing the samples into distilled water and suspended on 400-mesh TEM copper grid right before the TEM measurements. A plasma cleaning of 90 s was applied to remove the hydrocarbon and thin the carbon film.

⁷Z. Gai, B. Wu, J. P. Pierce, G. A. Farnan, D. J. Shu, M. Wang, Z. Zhang, and J. Shen, *Phys. Rev. Lett.* **89**, 235502 (2002).

⁸Micro-electron diffraction was performed using a 50 m aperture setting. The diffraction pattern was calibrated using a silicon $\langle 110 \rangle$ pattern.

⁹The 1 keV peak in the experimental spectra is the Cu *L* line. In order to get proper background around the Fe peak, a high concentration of copper is modeled. The measured Cu peaks are fluoresced from the TEM copper grid bars, therefore, the measured *K* to *L* ratios are $^\circ$ off, which is quite different from the simulated value.

¹⁰K. Reichelt, *J. Cryst. Growth* **35**, 55 (1976).

¹¹F. Liu, *Phys. Rev. Lett.* **89**, 246105 (2002).